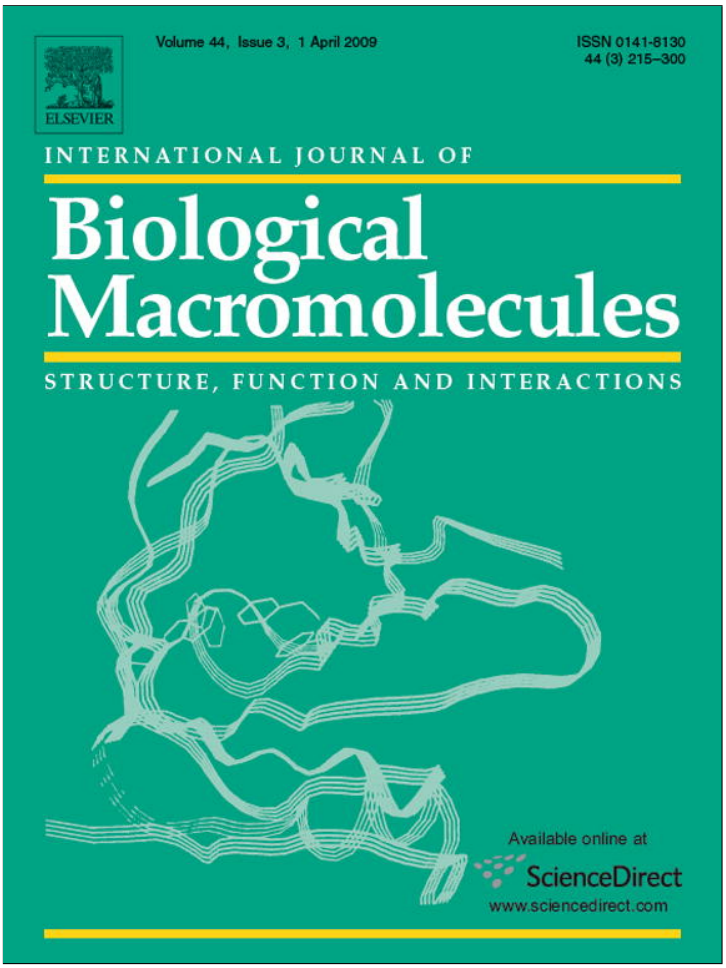

International Journal of Biological Macromolecules 44 (2009) 249–256

Contents lists available at ScienceDirect

International Journal of Biological Macromolecules

journal homepage: www.elsevier.com/locate/ijbiomac

Synthesis of novel pH-sensitive chitosan graft copolymers and micellar solubilization of paclitaxel

Hongxia Li[a,b,1], Jia Liu[a,1], Song Ding[a], Can Zhang[a,*], Wenbin Shen[c], Qidong You[d,*]

[a] Centre for Drug Discovery, China Pharmaceutical University, Nanjing 210009, PR China
[b] School of Pharmaceutical Science, Jiangsu University, Zhenjiang Jiangsu 212013, PR China
[c] Center for Instrumental Analysis of CPU, China Pharmaceutical University, Nanjing 210009, PR China
[d] Department of Medicinal Chemistry, China Pharmaceutical University, Nanjing 210009, PR China

ARTICLE INFO

Article history:
Received 26 November 2008
Received in revised form 16 December 2008
Accepted 17 December 2008
Available online 25 December 2008

Keywords:
Chitosan
pH-sensitive
Polymeric micelles
Hydrolysis
Paclitaxel

ABSTRACT

Herein, highly pH-sensitive graft copolymers, *N*-octyl-*N*-(2-carboxylbenzoyl) chitosan derivatives, were synthesized and characterized by FTIR, ^{1}H NMR, ^{13}C NMR, differential scanning calorimetry and X-ray diffraction spectrometry. The polymers can form micelles solublizing paclitaxel, with critical micellar concentrations ranged from 0.07 to 0.32 mg/ml, drug-loading rate ranged from 30.7% to 65.3% and entrapment efficiency ranged from 44.2% to 61.4%. Additionally, the result shows that the micelles display highly sensitivity to mildly acidic pH while reasonably stable at physiologic pH, which might pave the way for building pharmaceutical nanocarriers specifically releasing cargo at certain pathological sites of body.

1. Introduction

Polymeric micelles as drug delivery system associated with solubilization of low-solubility drugs and potentials for tumor targeting and controlled drug release have triggered considerable interests in recent years [1–4]. They are able to selectively accumulate in the tumor tissues depending on enhanced permeability and retention (EPR) effect and internalized by tumor cells usually vie endocytosis. In these cases, the micelles end up in the acidic environment (pH 5.0–5.5) of endosomes and lysosomes. The pH signal in these acidic organelles delivers aid to the pharmaceutical scientists in designing pH-responsive micelles [5,6]. Hrubý et al. had present a novel pH-sensitive micellar drug delivery systems based on hydrazone-bound doxorubicin [7]. V.P. Torchilin et al. developed double-targeted pH-responsive micelles with protective PEG chains by inserting the pH-sensitive hydrazone bond between PEG and PE in order to prevent the damage of target moieties including monoclonal antimyosin antibody 2G4, biotin and TAT peptide in vivo. Due to the acidic hydrolysis of PEG-Hz-PE at lower pH values (pH 5.0–6.0), the micelles lost their protective PEG, presenting enhanced targeted ability and effectively internalized efficiency [8].

Chitosan, a natural aminopolysaccharide obtained by hydrolysis of chitin, has been studied as a pharmaceutical carrier for drug delivery because of its favorable biological properties such as biocompatibility, biodegradability, positive charge, nontoxicity and bioadhesivity [9]. By grafting the hydrophobic and hydrophilic segments to chitosan backbone would give rise to the amphiphilic graft copolymers, which can form nanoscopic core–shell structures above the critical micellar concentration (CMC) physically incorporating varies hydrophobic drugs [10,11]. The chitosan-based amphiphilic polymer *N*-octyl-*O*-sulfate chitosan was reported to be a potent and safe polymeric material to load paclitaxel, improving drug solubility, prolonging drug circulation time, and reducing drug toxicity in vitro [12–14]. However, the problem of polymeric micelles associated with an absence of adequate drug release upon micelle accumulation in the tumor tissues, which is owe to excessive drug retention in micelle core, is usually revealed by clinical trials. One approach to conquer this is the application of pH-sensitive components that cause micelle destabilization in a specially controlled manner thus increasing the selectivity and efficiency of drug delivery to target cells. A protonation of a polybase poly(L-histidine) in the hydrophobic core of mixed PEG–poly(L-histidine)/PEG–PLLA micelles in the tumor cells resulted in destabilization of micelle cores and facile drug release in response to the acidic environment [15].

Amides with neighboring carboxylic acid groups were reported to exhibit pH-dependent hydrolysis. The amide of the secondary

* Corresponding authors. Tel.: +86 25 85333041; fax: +86 25 85333041.
E-mail address: zhangcan@cpu.edu.cn (C. Zhang).
[1] Both authors contributed equally to this work.

0141-8130/$ – see front matter © 2008 Elsevier B.V. All rights reserved.
doi:10.1016/j.ijbiomac.2008.12.011

amine almost instantly hydrolyzed at pH 5, slightly slower at pH 6, but only 50% even after 60 h at pH 7.4 [16]. In this article, we developed a pH-sensitive drug delivery system by modifying chitosan with amide linkage for the delivery of anti-cancer drug paclitaxel. The pH-sensitive polymeric micellar was able to release their contents in response to acidic pH within the endosomal system while remaining stable in plasma, thus improving the cytoplasmic delivery of paclitaxel after endocytosis. The amphiphilic acylated chitosan has been synthesized by the introduction of the octyl and carboxylbenzoyl groups to part of amino groups of chitosan. The chemical structure of *N*-octyl-*N*-(2-carboxylbenzoyl) chitosan (OCBCS) was confirmed by FTIR, ^{1}H NMR, ^{13}C NMR, elemental analysis, differential scanning calorimetry (DSC) and X-ray diffraction spectrometry (XRD) techniques. Transmission electron microscopy (TEM) techniques were exploited to evaluate the micelle-forming properties. The pH sensitivity of the polymeric micelle was evaluated by exploiting spectrophotometer, and proved to be stable in neutral solution while highly sensitive to mild acidic environment. In conclusion, this work would necessary for the further study on designing intelligent drug delivery systems.

2. Method

2.1. Materials

Chitosan was provided by Nantong Shuanglin Biochemical Co. Ltd. (China), with a degree of deacetylation of 92% (DA = 8%) and viscosity average molecular weight of 70,000 Da. Pyrene was purchased from Fluka Company (>99%). Paclitaxel was supplied by Taihua Natural Plant Pharmaceutical Co. Ltd. (China). All commercially available solvents and reagents were used without further purification.

2.2. Synthesis of amphiphilic chitosan derivative

N-octyl-*N*-(2-carboxylbenzoyl) chitosan derivatives were prepared by introducing an octyl group to NH_2 on C2 of glucosamine unit in chitosan followed by a different degree of *N*-acylated as shown in Scheme 1.

2.2.1. Preparation of N-octyl chitosan (NOC) [10]

Chitosan (2.0 g, 12 mmol as monosaccharide residue containing 11 mmol amino groups, 70,000 Da) was suspended in 60 ml of methanol solution with stirring at room temperature, and then octanal (5.3 ml, 33 mmol) was added to the reaction mixture. After 8 h, KBH_4 (2 g, 37 mmol) was slowly added to the solution in batch. After a further 24 h of continuous stirring, the reaction solution was neutralized with aqueous 1 M HCl solution, and the product was precipitated with methanol. The precipitate was filtered and repeatedly washed with methanol and water. The product, *N*-octylchitosan (NOC-2) was dried under vacuum at 60 °C overnight.

NOC-1, NOC-3, NOC-4 and NOC-5 were prepared following the same procedures using the chitosan (70,000 Da) as starting material by reacting 2, 5, 60 and 72 h, respectively.

2.2.2. Synthesis of N-octyl-N-(2-carboxylbenzoyl) chitosan derivatives

NOC-2 (0.5 g, 0.68 mmol) was dissolved in 25 ml of dimethyl sulfoxide (DMSO) solution with stirring at room temperature. Phthalic anhydride (0.4 g, 2 mmol) was slowly added to the solution in batch, and this mixture was heated to 80 °C with stirring. After 24 h of reaction, the reaction solution was neutralized with aqueous 20% NaOH solution to pH 10 at 0 °C, and the filtrate solution was dialyzed against distilled water for 5 days using a membrane obtained from Sigma with a molecular weight cut-off range of 10,000. The solution was lyophilized, and 0.34 g of *N*-octyl-*N*-(2-carboxylbenzoyl) chitosa (OCBCS-2) powder was obtained.

OCBCS-1, OCBCS-3, OCBCS-4, and OCBCS-5 were prepared following the same procedures using the NOC-1, NOC-3, NOC-4 and NOC-5 as starting materials, respectively.

2.3. Characterization of chitosan derivatives and measurement of physical properties

^{1}H NMR and ^{13}C NMR spectra were performed on a Bruker (AVACE) AV-300 spectrometer. Chitosan was dissolved in the mixed solvent of D_2O and CF_3COOD, and chitosan derivatives were dissolved in D_2O.

FTIR spectra were recorded on Fourier-transform infrared spectrometer (Nicolet 2000) in KBr discs.

Elemental analysis was determined using an Element Vario EL III analyzer. Data from elemental analysis was used to calculate the degree of *N*-alkyl substitution.

XRD was obtained by using XD-3A powder diffraction meter with Cu Kα radiation in the range of 5–40 °C (2θ) at 40 kV and 30 mA.

The results of DSC were obtained with NETZSCH DSC 204 equipment respectively. The temperature range is 30–500 °C and heating rate of 20 °C/min.

Turbidity measurements were measured with 752N UV–VIS spectrophotometer (Shanghai Huxi Analysis Instrument Factory Co. Ltd.).

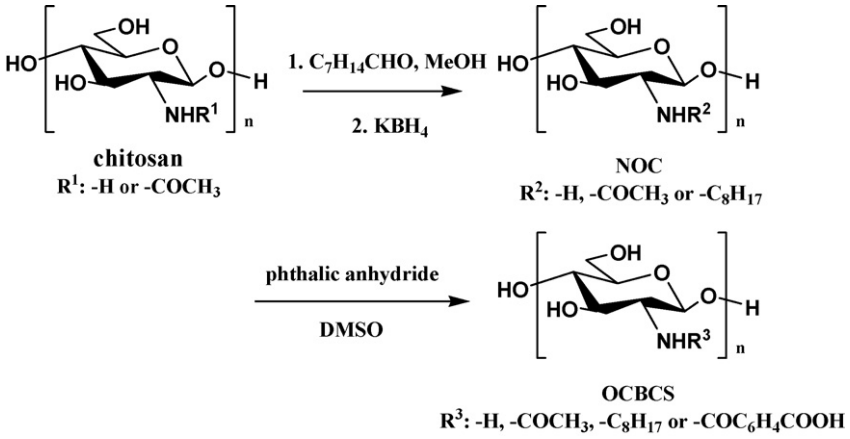

Scheme 1. Synthesis route of OCBCS.

2.4. Measurement of CMC

The CMC of the OCBCS were determined by using surface tension method [17]. Briefly, prepare 30 ml of various concentrations of OCBCS solutions (0.05–0.45 mg/ml) in the 50 ml beakers, then the sample solutions were left overnight to equilibrate at room temperature (25 °C). Surface tension of each solution was measured on DCAT 21-Tensiometer (Dataphysics Company, Germany) using the plat plate method.

2.5. Preparation of paclitaxel-loaded chitosan derivative micellar solutions

Paclitaxel-loaded chitosan derivative micellar solutions were prepared by dialysis [18]. Briefly, OCBCS 12 mg was dissolved in 3 ml water. 5.7 mg of paclitaxel was dissolved in 0.25 ml ethanol (the feeding ratio of the drug to copolymer was 1:2), and then the paclitaxel solution was injected into OCBCS solution with stirring at room temperature, followed by dialysis against distilled water about six hours using a dialysis membrane (MWCO 10,000). The micellar solution was filtered with a 0.8 μm pore-sized microfiltration membrane.

2.6. Measurement of paclitaxel concentration in OCBCS derivatives micellar solutions

The concentration of paclitaxel in the micellar solution was determined by HPLC (HP1100, Agilent, USA). The mobile phase was a mixture of methanol and water (75:25, v/v). The column was a Diamohsile C18 (4.6 mm × 250 mm, 5 μm, Dikma, Beijing, China). The flow rate was 1.0 ml/min, the detection wavelength was 227 nm (UV detector, HP1100, Agilent, USA), the column temperature was 25 °C and the injected volume of the sample was 20 μl.

2.7. Characterization of polymeric micelle systems

Size of the polymeric micelles was measured using a Zetasizer 3000HS instrument (Malvern Instruments, Malvern, UK) with 633 nm He–Ne lasers at 25 °C. TEM analysis was performed using the micellar solution with JEM-200CX (JEOL Ltd., Japan). The micellar solution was placed on a copper grid coated with framer film.

2.8. In vitro pH-dependent hydrolysis of chitosan graftpolymer [19]

The pH sensitivity of the chitosan graftpolymer was evaluated by using the spectrophotometer. To assess the effect of the hydrolysis of the amide group in OCBCS, we monitored the changes of transmittance at λ = 560 nm of aqueous polymer solutions within a wide pH range. The OCBCS-2 sample was dissolved in phosphate buffer solutions of different pH values (i.e. pH values 5.0, 6.0, 6.5, 7.0 and 7.4). The solution pH was measured with a Delta 320 pH meter equipped with a Mettler-Toledo instrument (Shanghai).

3. Results and discussion

3.1. Synthesis and characterization of chitosan derivatives

The synthetic route of OCBCS was briefly summarized in Scheme 1.

The structure of these graft copolymers was characterized by ^{1}H NMR spectra (Fig. 1), ^{13}C NMR spectra (Fig. 2) and FTIR spectra (Fig. 3). Compared with chitosan, the ^{1}H NMR spectrum of OCBCS (Fig. 1) showed new-emerged peaks at δ (ppm) 0.8–1.85 which attributed to the -CH_2 and -CH_3 of the long-chain alkyl group, the results certified that the chitosan derivative carried *N*-octyl groups.

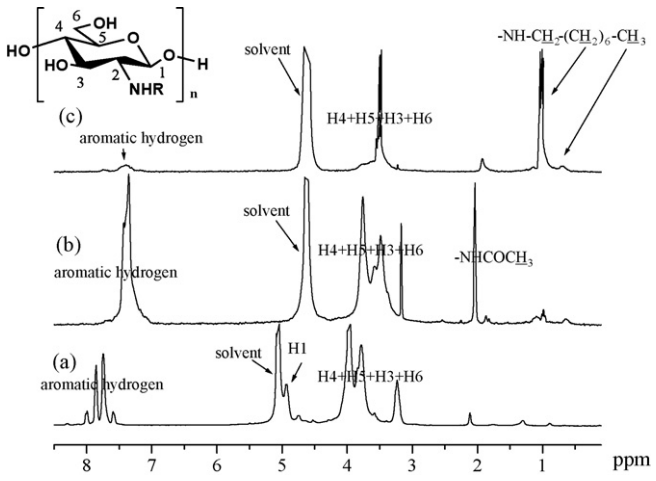

Fig. 1. ^{1}H NMR (D_2O) spectra of (a) OCBCS-1, (b) OCBCS-2, and (c) OCBCS-5.

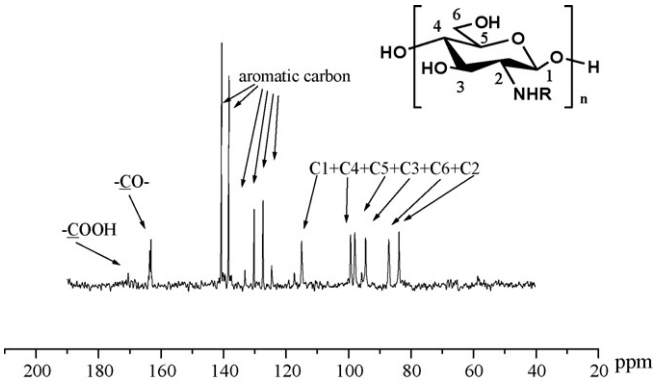

Fig. 2. ^{13}C NMR spectra of OCBCS-1.

And the peaks at δ (ppm) 7.2–7.9 attributed to the aromatic carbon of the *N*-carboxylbenzoyl groups indicating the successful graft of these segments onto chitosan backbone. The degree of octyl substation onto OCBCS was 13.4%, 36.4% and 64.2% respectively. And that of the carboxylbenzoyl group was 92.3%, 80.8% and 52.9% as calculated by elemental analysis. It was found that with DD of octyl group increased from 13.4% to 64.2%, the carboxylbenzoyl group on chitosan chain decreased.

Fig. 2 showed the ^{13}C NMR spectra of chitosan and OCBCS-1. The signals of chitosan at δ (ppm) 85.6 (C2), 87 (C6), 93 (C3), 96 (C5),

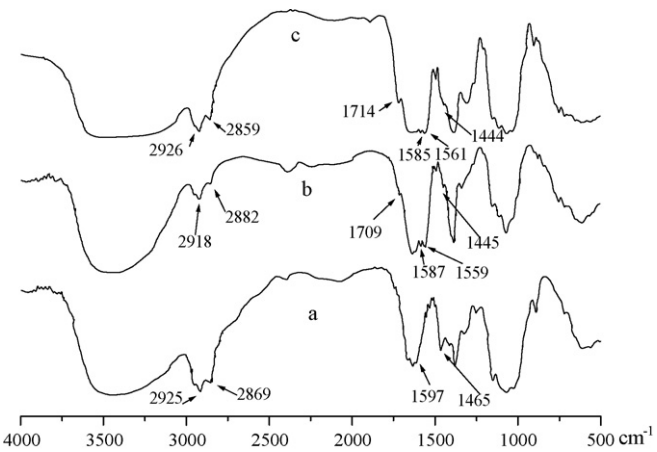

Fig. 3. FTIR spectra of (a) NOC-2, (b) OCBCS-2, and (c) OCBCS-5.

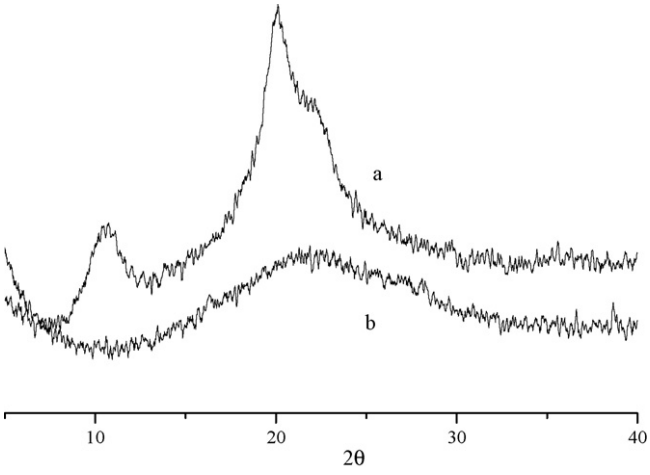

Fig. 4. XRD patterns of (a) NOC-2 and (b) OCBCS-2.

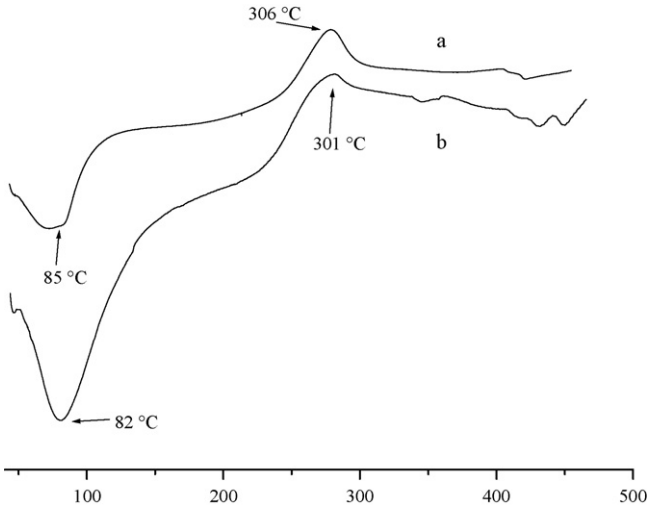

Fig. 5. DSC thermograms of (a) NOC-2 and (b) OCBCS-2.

98 (C4) and 115 (C1) were detected. Compared with chitosan, the ^{13}C NMR spectrum of OCBCS-1 showed the signals at δ (ppm) 170 and 165 assigned to the carboxyl carbon (-COOH, -CO) of the *N*-carboxylbenzoyl groups, and the signals at δ (ppm) 124, 128, 130.5, 132.3, 138.6 and 140.5 attributed to the aromatic carbon of the *N*-carboxylbenzoyl groups, respectively. Meanwhile, the peaks at δ (ppm) 23.9 and 33.5 which were assigned to methyl carbon and methene carbon of the *N*-octyl groups were not obvious because DD of octyl group were only 13.4%. These results indicated that OCBCS contained *N*-octyl groups and *N*-carboxylbenzoyl groups.

FTIR analysis was performed to evaluate the *N*-alkyl substitution. Fig. 3 shows the FTIR spectra of NOC and OCBCS. Chitosan had the strongest absorbance at 1597 cm^{-1}, which indicated the presence of the NH_2 group on C2 of the glucosamine unit. The intensity of this specific NH_2 signal was significantly decreased upon introducing the *N*-octyl group and was hardly observed for OCBCS. In comparison of the FTIR spectra of chitosan and NOC, introducing the *N*-alkyl into the molecule increased intensities of peaks at 2869 and 2925 cm^{-1}, suggesting the presence of *N*-alkyl substitution [20]. Furthermore, the intensity of these peaks was greater in the FTIR spectra of OCBCS-5 than that observed for OCBCS-2 under the same experimental conditions, indicating the additional *N*-alkyl substitution (Fig. 3b and c). These data suggest the presence of methyl and long alkyl groups on nitrogen at the C2 position of the glucosamine unit in chitosan molecules. New peaks were observed at about 1450 cm^{-1} in the FTIR spectra of NOC and OCBCS.

3.2. Physical properties of modified chitosan

XRD and DSC spectrometry were employed to study the physical properties of chitosan and its derivatives.

XRD was conducted for NOC and OCBCS to further evaluate their crystallization behaviors. Two reflection falls at 2θ of 11° and 20° were observed in the X-ray diffraction spectrum of NOC (Fig. 4a), whereas OCBCS only had one broad peak at 2θ of about 22° (Fig. 4b). It is well accepted that the reflection fall at 2θ of 11° reflects the presence of crystal form I and the strongest reflection at 2θ of 20° corresponds to crystal form II. The data in Fig. 4 indicted that introduction of octyl and carboxylbenzoyl group to chitosan main chain decreased their ability of forming intermolecular hydrogen bonds. It also suggested that OCBCS was amorphous, which was further supported by their DSC thermograms under the experimental condition.

DSC thermograms of NOC and OCBCS are shown in Fig. 5. The spectrum of NOC shows a broad endothermic peak around 85 °C and a sharp exothermic peak at 306 °C. The former endothermic peak may be caused by the water vapor that the NOC contained and some of the polymer had low molecular weight. The latter may be attributed to the decomposition of chitosan. The endothermic peak of OCBCS around 82 °C may be caused by the loss of water and moisture content of the polysaccharide, respectively. The broad exothermic peak at 301 °C corresponds to its thermal decomposition. The result indicated that the structure of chitosan chains has been changed by the introduction of the carboxylbenzoyl group and the ability of crystallization was decreased.

3.3. Measurement of CMC

Representative plots of surface tension versus concentration at 25 °C were shown in Fig. 6, which presented that the surface tension decreases with the concentration of copolymers of different degree of substitution (DS) of octyl group increased. In each case, the surface tension drops abruptly to a minimum. The CMC values were calculated by the crossover point at which the surface tension reaches this minimum. All the CMC values are listed in Table 1. According to these results, the higher DS of octyl group, the lower the CMC value was. To reveal the relationship of CMC and the structure of OCBCS, three structure parameters, DS of octyl group, carboxylbenzoyl group and CS unit by mole per kilogram (mol/kg), were introduced. The different degree of substitution (mol/kg) could be calculated by the following equations. The obtained values

Table 1
The DS of octyl group, carboxylbenzoyl group and chitosan(CS) unit, CMC, log CMC of chitosan derivatives.

DS of octyl group (%)	DS of octyl group (mol/kg)	DS of carboxylbenzoyl group (mol/kg)	DS of CS unit (mol/kg)	CMC (mg/ml)	log CMC
28	1.00	2.20	3.46	0.32	−0.49
36	1.13	2.50	3.10	0.19	−0.72
43	1.32	2.47	3.06	0.13	−0.88
53	1.69	2.05	3.19	0.14	−0.85
64	2.05	1.69	3.20	0.07	−1.15

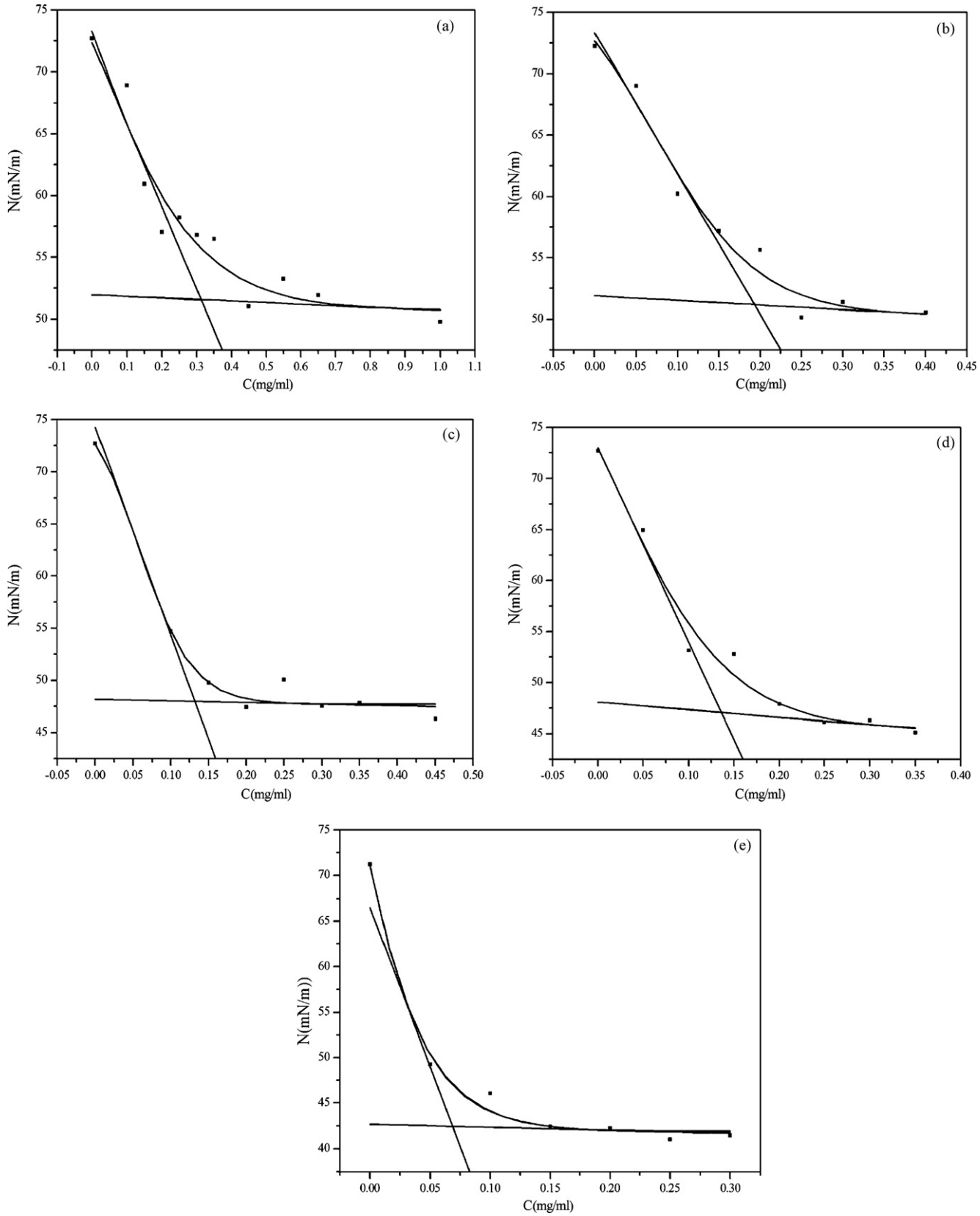

Fig. 6. The plots of surface tension versus concentration for copolymers of different DS of octyl group in aqueous solution. The error of surface tension value is ±0.3 mN/m (a: 28%, b: 36%, c: 43%, d: 53%, e: 64%).

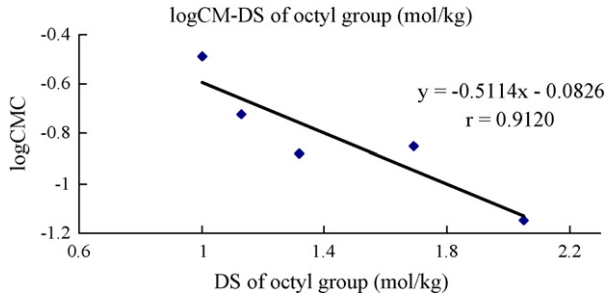

Fig. 7. The linear regression curves of log CMC versus DS of octyl group.

of four structure parameters were listed in Table 1.

$$\text{DS of octyl group (mol/kg)} = 1000 \times \frac{\text{DS of octyl group}}{\text{MW}_{(\text{OCBCs unit})}} \quad (1)$$

$$\text{DS of carboxylbenzoyl group (mol/kg)} = 1000 \times \frac{\text{DS of carboxylbenzoyl group}}{\text{MW}_{(\text{OCBCs unit})}} \quad (2)$$

$$\text{DS of octyl group (mol/kg)} = \frac{1000}{\text{MW}_{(\text{OCBCs unit})}} \quad (3)$$

where $\text{MW}_{(\text{OCBCs unit})}$ represented the molar weight of OCBCs unit.

Fig. 7 showed the result of linear regression with log CMC to DS of octyl group by mole per kilogram, and the absolute values of correlation coefficients (r) were larger than 0.9, which suggested that it was linear relative.

3.4. Characterization of paclitaxel-loaded chitosan derivative micelles

Table 2 listed paclitaxel concentration, drug-loading rate, entrapment efficiency, particle size and zeta potential of paclitaxel-loaded micelles, and drug-loading rate and entrapment efficiency could be calculated by Eqs. (4) and (5).

$$\text{drug-loading rate} = \frac{C \times V}{W_{\text{freeze-dried micelle}}} \times 100\%; \quad (4)$$

$$\text{entrapment efficiency} = \frac{C \times V}{W_{\text{paclitaxel}}} \times 100\%; \quad (5)$$

where C, V, $W_{\text{freeze-dried micelle}}$ and $W_{\text{paclitaxel}}$ represented the paclitaxel concentration of micellar solution, the volume of micellar solution, the weight of freeze–dried micelle and the weight of paclitaxel added, respectively.

Drug loading content and encapsulation efficiency are two critical characteristics for evaluating the capacity of a selected polymer to entrap and carry a selected drug. In our study, all the OCBCs had high paclitaxel concentrations (0.82–1.12 mg/ml). The encapsulation efficiency and drug-loading rate of micelles preparation with an octyl substitution degree of 28–64% ranged from 44.2%, 30.7% to 61.4%, 54.9%, respectively (Table 2). However, since the graftpolymers which had the higher DS of octyl group exhibited the lower solubility, for consideration of both the solubility and drug-loading rate, the soluble graftpolymer with the octyl DS of 36%, whose drug-loading rate reaches 1.12 mg/ml, was selected for further research.

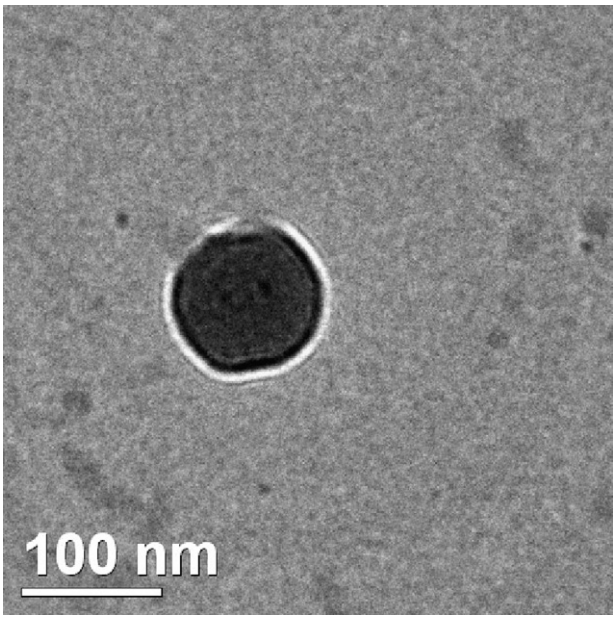

Fig. 8. TEM of paclitaxel in OCBCS-2 micelles.

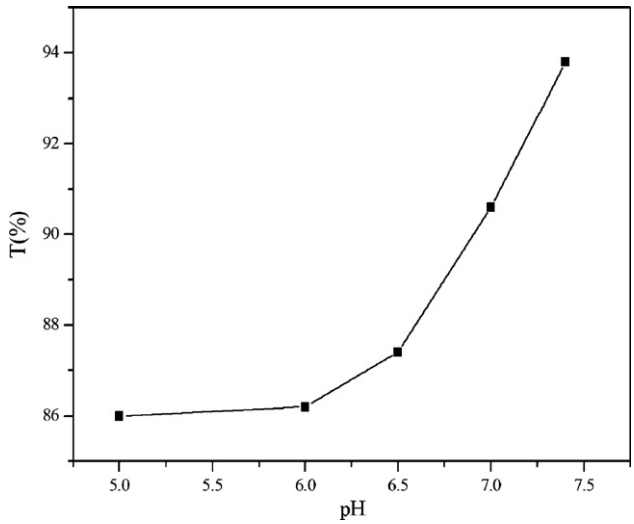

Fig. 9. Changes of the transmittance (T) as a function of the OCBCS-2 solution pH.

It has been observed that solvent used to dissolve drug molecules may significantly affect micelle formation and drug-loading rate. The effect of relative amount of ethanol and water on drug loading content was investigated in our work. When increased the relative radio of ethanol to water to 1:12, paclitaxel would all precipitate from the micelle systems during dialysis course, the copolymer cannot entrap PTX steadily. This may be due to the inter-

Table 2
Paclitaxel concentration, drug-loading rate, entrapment efficiency and particle size of paclitaxel-loaded micelles ($n = 3$).

DS of octyl group (%)	Paclitaxel concentration (mg/ml)	Drug-loading rate (%, w/w)	Entrapment efficiency (%)	Particle size (nm)	Zeta potential (mV)
28	1.01 ± 0.06	34.6 ± 2.1	53.4 ± 4.6	163.7 ± 5.3	−18.5 ± 0.4
36	1.19 ± 0.10	37.1 ± 2.1	61.4 ± 4.5	180.8 ± 10.9	−21.8 ± 4.7
43	0.82 ± 0.08	31.3 ± 2.9	51.4 ± 3.9	158.7 ± 6.4	−18.9 ± 3.9
53	0.91 ± 0.09	30.7 ± 0.4	44.2 ± 3.9	147.8 ± 5.0	−22.2 ± 3.6
64	1.02 ± 0.07	54.9 ± 1.8	57.6 ± 8.7	100.5 ± 1.5	−17.9 ± 3.3

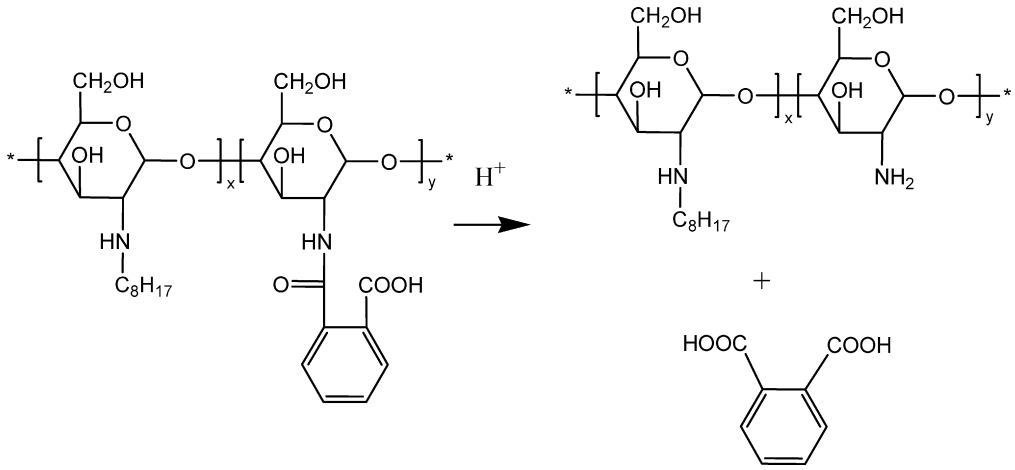

Scheme 2. Hydrolyze route of OCBCS at acidic pH.

ference of ethanol on micelle formation and its ability to reduce PTX diffusion into the hydrophobic core of the micelles. Therefore, it is recommended that amount of organic solvent should be minimized for dissolving the drug and their residues should be removed completely after the drug is loaded.

The TEM micrograph of the OCBCS-2 micelles was presented in Fig. 8, showing that OCBCS-2 was able to form nanoscale near-spherical micelles with slight deformation and aggregation.

3.5. *In vitro pH-dependent hydrolysis of OCBCS [19]*

The pH-sensitive polymeric micelles based on OCBCS in our work are expected to be stable in circulation, while rapidly release the loads once entering into endosomes or lysosomes of tumor cells in response to acidic environment (pH ~ 5.0). However, it is well established that the extracellular pH of tumor cells is slightly lower (pH 6.3–6.8) than the surrounding tissues and blood (pH 7.5) [21–23], which might cause the premature release of the drugs outside the targeted cells and undermine our expectation. As a result, a wild range of pH value (5.0, 6.0, 6.5, 7.0 and 7.4) were included in the experiment (Fig. 9).

The pH sensitivity of the chitosan graftpolymer was evaluated by using the spectrophotometer. Because the hydrolysis of the amide group in OCBCS (Scheme 2) would lead to the formation of NOC that is insoluble in acidic solution, the transmittances of sample solution in our study decrease with the increased degree of hydrolysis. Solution of OCBCS-2 sample at pH 7.4 remained transparent to light (94.5% transmittance), whereas the transmittance of the OCBCS-2 solution at pH 5.0 decreased sharply (85.5% transmittance), suggesting that the hydrolyze rate of OCBCS sample was larger in phosphate buffer solution pH 5.0 than at pH 7.4. As a consequence, the micelles formed by OCBCS were found to be highly sensitive to acidic pH and reasonably stable under physiologic pH.

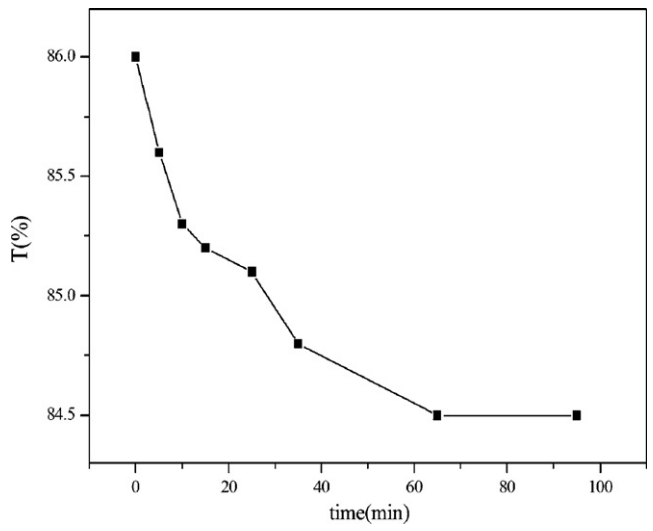

Fig. 10. Changes of the transmittance (*T*) as a function of the time at OCBCS-2 solution pH 5.

The hydrolysis process of OBCBS was studied over the period of time in PBS at pH 5.0 (37.4 °C). Fig. 10 showed with the extension of the time, the transmittance drop, and slow downward trend after 60 min. The results indicate that the hydrolyze rates of OCBCS in PBS were mainly depended upon the time. Advanced researches are ongoing to provide more evidences to confirm the fantastic possibility and feasibility for the novel pH-sensitive drug carrier to target solid tumors punctually.

4. Conclusions

A series of novel pH-sensitive graft copolymer, *N*-octyl-*N*-(2-carboxylbenzoyl) chitosan derivatives were prepared. The chemical structures of chitosan derivatives and some of their physical properties were characterized by FTIR, ^{1}H NMR, ^{13}C NMR, elemental analysis, DSC, XRD and TEM techniques. The amphiphilic OCBCS would self-assemble to form micelles in the aqueous solution and had good solubilization ability of paclitaxel. The CMCs of the modified chitosans were found to be 0.07–0.32 mg/mL, and the log CMC was linear relative to DS of octyl group by mole per kilogram. This study shows that the micelles formed by these graft copolymers are stable in neutral solution (pH 7.4) while highly sensitive to mild acidic environment (pH 5.0–6.0). Further research on the drug release characteristic is undertaken in our lab and the results will be reported later.

Acknowledgments

This study is financially supported by National Natural Science Foundation of China (30772662), Program for New Century Excellent Talents in University (NCET-06-0499), Ministry of Education key project (107062), and 111 Project from the Ministry of Education of China and the State Administration of Foreign Expert Affairs of China (No. 111-2-07).

References

[1] P. Opanasopit, T. Ngawhirunpat, T. Rojanarata, C. Choochottiros, S. Chirachanchai, European Journal of Pharmaceutical Sciences 30 (2007) 424–431.
[2] S.C. Chen, Y.C. Wu, F.L. Mi, Y.H. Lin, L.C. Yu, H.W. Sung, Journal of Controlled Release 96 (2004) 285–300.
[3] J. Wu, Z.G. Su, G.H. Ma, International Journal of Pharmaceutics 315 (2006) 1–11.
[4] N.M. Alves, J.F. Mano, International Journal of Biological Macromolecules 43 (2008) 401–414.
[5] J. Du, J. Dai, J.L. Liu, T. Dankovich, Reactive & Functional Polymers 66 (2006) 1055–1061.
[6] V.A. Sethuraman, K. Na, Y.H. Bae, Biomacromolecules 7 (2006) 64–70.
[7] M. Hrubý, Č. Koňák, K. Ulbrich, Journal of Controlled Release 103 (2005) 137–148.
[8] R.M. Sawant, J.P. Hurley, S. Salmaso, A. Kale, E. Tolcheva, T.S. Levchenko, V.P. Torchilin, Bioconjugate Chemistry 17 (2006) 943–949.
[9] X.H. Wang, F.Z. Cui, Q.L. Feng, J.C. Li, Y.H. Zhang, Journal of Bioactive and Compatible Polymers 18 (2003) 453–467.
[10] C. Zhang, Y. Ding, L.L. Yu, Q.N. Ping, Colloids and Surfaces B: Biointerfaces 55 (2007) 192–199.
[11] Z. Yao, C. Zhang, Q.N. Ping, L.L. Yu, Carbohydrate Polymers 68 (2007) 781–792.
[12] C. Zhang, Q.N. Ping, H.J. Zhang, Colloids and Surfaces B: Biointerfaces 39 (2004) 69–75.
[13] C. Zhang, G.W. Qu, Y j Sun, T. Yang, Z. Yao, European Journal of Pharmaceutical Sciences 33 (2008) 415–423.
[14] C. Zhang, G.W. Qu, Y.J. Sun, X.L. Wu, Z. Yao, Q.L. Guo, Biomaterials 29 (2008) 1233–1241.
[15] E. Lee, H.J. Shin, K. Na, Y.H. Bae, Journal of Controlled Release 90 (2003) 363–374.
[16] P.S. Xu, E.A. Van Kirk, Y.H. Zhan, W.J. Murdoch, M. Radosz, Y.Q. Shen, Angewandte Chemie International Edition 46 (2007) 4999–5002.
[17] X. Xin, G.Y. Xu, Z.Q. Zhang, Y.J. Chen, F. Wang, European Polymer Journal 43 (2007) 3106–3111.
[18] G.S. Kwon, M. Naito, M. Yokoyama, T. Okano, Y. Sakurai, K. Kataoka, Pharmaceutical Research 12 (1995) 192–195.
[19] M.J. Tiera, X.P. Qiu, S. Bechaouch, Q. Shi, Biomacromolecules 7 (2006) 3151–3156.
[20] F. Li, W.G. Liu, K.D. Yao, Biomaterials 23 (2002) 343–347.
[21] M. Stubbs, P.M.J. McSheehy, J.R. Griffiths, C.L. Bashford, Molecular Medicine Today 6 (2000) 15–19.
[22] R.K. Jain, Journal of Controlled Release 74 (2001) 7–25.
[23] A. Asokan, M.J. Cho, Journal of Pharmaceutical Sciences 91 (2002) 903–913.